Journal of Biomolecular NMR **30:** 431–442, 2004.

Determination of protein rotational correlation time from NMR relaxation data at various solvent viscosities

Denis S. Korchuganov, Ivan E. Gagnidze, Elena N. Tkach, Alexey A. Schulga, Mikhail P. Kirpichnikov & Alexander S. Arseniev*

Shemyakin-Ovchinnikov Institute of Bioorganic Chemistry, Russian Academy of Sciences, ul. Miklukho-Maklaya, 16/10, Moscow, 117997, Russia

Received 24 September 2004; Accepted 30 September 2004

Key words: barnase, correlation time, glycerol, NMR relaxation, protein dynamics, viscosity

Abstract

An accurate determination of the overall rotation of a protein plays a crucial role in the investigation of its internal motions by NMR. In the present work, an innovative approach to the determination of the protein rotational correlation time τ_R from the heteronuclear relaxation data is proposed. The approach is based on a joint fit of relaxation data acquired at several viscosities of a protein solution. The method has been tested on computer simulated relaxation data as compared to the traditional τ_R determination method from T_1/T_2 ratio. The approach has been applied to ribonuclease barnase from *Bacillus amyloliquefaciens* dissolved in an aqueous solution and deuterated glycerol as a viscous component. The resulting rotational correlation time of 5.56 ± 0.01 ns and other rotational diffusion tensor parameters are in good agreement with those determined from T_1/T_2 ratio.

Introduction

NMR relaxation is the richest source of experimental information on protein dynamics and can reveal details on the atomic level. By analysing backbone amide nitrogen relaxation, the global picture of the dynamics of a protein can be revealed. Standard relaxation data set consists of three relaxation values per magnetic field strength, the ^{15}N–^{1}H steady-state NOE, and the ^{15}N T_1 and T_2 relaxation times. The most popular method of the analysis of backbone ^{15}N relaxation data in terms of protein motions is the model-free approach proposed originally by Lipary and Szabo (1982) and extended by Clore et al. (1990). This theory describes internal motions in terms of generalised order parameters and effective correlation times without any assumptions about the nature of the motions.

There are two major difficulties associated with the model-free approach. The first one is that the model-free approach implicitly exploits the assumption that global diffusion of a protein and internal motions are not correlated. If internal and rotational motions are coupled, this assumption does not hold and the model-free approach is inapplicable (Tugarinov et al., 2001). The second problem is a certain ambiguity in the determination of the protein rotational correlation time τ_R from ^{15}N NMR relaxation data. If the intramolecular motions of most of the protein ^{15}N nuclei are fast ($\tau_e < 100$ ps), then the value of τ_R could be calculated from T_1/T_2 ratio (Tjandra et al., 1995). However, if the major part of the molecule is involved in internal motions with characteristic times close to overall correlation time, the value of τ_R

*To whom correspondence should be addressed. E-mail: aars@nmr.ru

obtained from the relaxation data even acquired on several spectrometers with different resonance frequencies will be underestimated (Korzhnev et al., 1997). The underestimated τ_R, when used in further calculations, leads to overestimated order parameters, underestimated correlation times of internal motions, and might result in an apparent consistency of the relaxation data with the simplest model assuming fast intramolecular motions. A possible way of solving the problem could be by using the relaxation data acquired for the same protein in different conditions in which the overall rotational correlation time is changed without affecting the internal motions.

A novel approach aimed at increasing the amount of experimental relaxation data by varying solvent viscosity has been proposed recently (Zeeb et al., 2003). This study, which considered solutions with different viscosities separately, has shown that fast internal motions are mainly independent of the viscosity. The increase in solvent viscosity has been achieved by adding various quantities of ethylene glycol to a protein solution. In the present work, we showed, by employing numerical methods that if internal protein motions are not affected by an additional viscous component, then it is possible to separate internal and overall motions by simultaneous analysis of relaxation data acquired at different viscosities. The approach was experimentally tested on extracellular ribonuclease barnase from *Bacillus amyloliquefaciens*, a small globular protein of 110 amino acid residues (Hartley, 1997), dissolved in an aqueous solution and deuterated glycerol as a viscous component.

Theory

Model-free analysis of relaxation rates

With the assumptions of the model-free approach the correlation function $C(t)$ of the ^{15}N–^{1}H bond vector can be factorized into a product of internal $C_I(t)$ and overall $C_O(t)$ parts (Lipary and Szabo, 1982):

$$C(t) = C_I(t)C_O(t). \quad (1)$$

The simplest model of the overall rotation is the isotropic rotational diffusion which leads to the single-exponential form of the correlation function $C_O(t)$:

$$C_O(t) = \exp(-t/\tau_R), \quad (2)$$

where τ_R is the overall rotational correlation time which is connected with the rotational diffusion coefficient D through the relation:

$$\tau_R = 1/(6D). \quad (3)$$

In the case of anisotropic rotational diffusion, the correlation function $C_O(t)$ is given by (Woessner, 1962):

$$\begin{aligned} C_O(t) = {} & A_1 \exp(-t/\tau_1) + A_2 \exp(-t/\tau_2) \\ & + A_3 \exp(-t/\tau_3) + A_4 \exp(-t/\tau_4) \\ & + A_5 \exp(-t/\tau_5), \end{aligned} \quad (4)$$

where coefficients A_1–A_5 can be calculated from the components D_x, D_y, D_z of the diffusion tensor, Euler's angles α, β, γ defining rotation from the structure coordinate frame to the coordinate frame where rotational diffusion tensor has a diagonal form, and directional cosines l, m and n of the ^{15}N–^{1}H vector with respect to the axes x, y and z of the structure coordinate frame as described elsewhere (Korzhnev et al., 2001). The corresponding time constants are defined as follows:

$$\begin{aligned} \tau_1 &= (4D_x + D_y + D_z)^{-1}, \\ \tau_2 &= (4D_y + D_x + D_z)^{-1}, \\ \tau_3 &= (4D_z + D_x + D_y)^{-1}, \\ \tau_4 &= [6(D + (D^2 - L^2)^{1/2})]^{-1}, \\ \tau_5 &= [6(D - (D^2 - L^2)^{1/2})]^{-1}, \end{aligned}$$

where $D = 1/3(D_x + D_y + D_z)$, $L^2 = 1/3(D_xD_y + D_xD_z + D_yD_z)$.

Rotational correlation time τ_R for the anisotropic rotation is defined through the components of the diffusion tensor in the manner analogous to the isotropic case (Equation 3):

$$\tau_R = 1/(6D) = 1/(2D_x + 2D_y + 2D_z). \quad (5)$$

If the protein spatial structure is known, the components of the diffusion tensor D_x, D_y, D_z, Euler's angles α, β, γ and directional cosines l, m, n could be computed numerically using the beads model approximation (for the review see Korzhnev et al., 2001). This method allows one to compute ratios D_x/D_z, D_y/D_z leaving only one adjustable parameter τ_R for accounting for the

rotational diffusion during model-free calculations even in the case of anisotropic rotation.

In order to account for the dependence of τ_R on the viscosity of a solution the translation diffusion coefficient D_t has to be measured. This allows one to express τ_R for the particular viscosity ($\tau_{R\eta}$) through the rotational correlation time in the 0%-glycerol solution τ_R using the relation (Orekhov et al., 1999, 2000)

$$\tau_{R\eta} = \tau_R(D_t/D_{t\eta}), \quad (6)$$

where $D_{t\eta}$ and D_t are translation diffusion coefficients in the solutions with and without glycerol respectively; $\tau_{R\eta}$ and τ_R are corresponding rotational correlation times. Thus we can use only one adjustable parameter τ_R for the whole set of experimental data with different viscosities. The Equation 6 is based on the assumption of linear dependence between rotational and translational diffusion, which is fully valid only for dilute solutions. High protein concentrations yield a linear attenuation of the translational diffusion rate (for the review see Korzhnev et al., 2001), but the ratio $D_t/D_{t\eta}$ remains to be independent of the protein concentration, and the Equation 6 still remains in force.

Five-exponential function (Equation 4) for the particular ^{15}N–^{1}H bond vector can be effectively approximated by a single exponent (Equation 2) if we replace τ_R in the Equation 2 by the effective rotational correlation time τ_{Reff} for this vector:

$$\tau_{Reff} = A_1\tau_1 + A_2\tau_2 + A_3\tau_3 + A_4\tau_4 + A_5\tau_5. \quad (7)$$

The distribution of τ_{Reff} for the particular ^{15}N–^{1}H bond vector over the set of protein structures (e.g. the set of NMR structures) reflects an uncertainty in the correlation function due to an uncertainty in the vector direction. Thus, it is convenient to use the standard deviation of τ_{Reff} over the set of protein structures as the measure of uncertainty in the ^{15}N–^{1}H vector direction in order to exclude residues with poorly defined orientation.

The original model-free approach (Lipary and Szabo, 1982) describes a single internal motion using two parameters S^2 and τ_e, where S^2 is the square of the generalised order parameter reflecting the amplitude of motion and τ_e is the effective correlation time reflecting the timescale of the motion. The extended theory (Clore et al., 1990) includes internal motions on two timescales with the faster of them described by the parameters S_f^2 and τ_f, and the slower by S_s^2 and τ_s. An additional term used in model-free analysis is R_{ex}, which is included to account for the relaxation due to a chemical exchange and is an indicator of motions on micro to millisecond timescales. Different types of internal motions can be characterized by various combinations of the model-free parameters. The combinations considered in the present study are model 1 $\{S^2\}$, model 2 $\{S^2, \tau_e\}$, model 3 $\{S_f^2, S_s^2, \tau_s\}$, model 4 $\{S^2, R_{ex}\}$, and model 5 $\{S^2, \tau_e, R_{ex}\}$.

If the parameters of internal and overall motions are known, the spectral density function $J(\omega)$ which is Fourier transform of $C(t)$ can be calculated for each ^{15}N–^{1}H vector. The relaxation times T_1, T_2 of ^{15}N nuclei and ^{15}N–^{1}H NOE are related to the spectral density function (Abragam, 1961)

$$\begin{aligned}
1/T_1 &= (d^2/4)[J(\omega_H - \omega_N) + 3J(\omega_N) \\
&\quad + 6J(\omega_H + \omega_N)] + c^2J(\omega_N) \\
1/T_2 &= (d^2/8)[4J(0) + J(\omega_H - \omega_N) \\
&\quad + 3J(\omega_N) + 6J(\omega_H) \\
&\quad + 6J(\omega_H + \omega_N)] + (c^2/6)[4J(0) \\
&\quad + 3J(\omega_N)] + R_{ex} \\
\mathrm{NOE} &= (d^2T_1/4)(\gamma_H/\gamma_N)[6J(\omega_H + \omega_N) \\
&\quad - J(\omega_H - \omega_N)],
\end{aligned}$$

where $d = (\mu_0 h\gamma_N\gamma_H/8\pi^2)\langle r_{NH}^{-3}\rangle$, $c = \omega_N\Delta\sigma/\sqrt{3}$, μ_0 is the permeability of free space; h is Planck's constant; γ_H and γ_N are the gyromagnetic ratios of ^{1}H and ^{15}N respectively; r_{NH} is the nitrogen-hydrogen bond length; ω_H and ω_N are the Larmor frequencies of ^{1}H and ^{15}N respectively; and $\Delta\sigma$ is the chemical shift anisotropy of ^{15}N nuclei.

Model evaluation and statistical analysis

In order to extract parameters of overall (τ_R and diffusion tensor parameters) and internal (e.g., models 1–5) motions, the experimental relaxation rates and NOEs are fitted to the theoretical values by minimizing the per residue loss function χ^2:

$$\chi^2(\zeta) = \sum_{i=1}^{N} \frac{(V_i^{th}(\zeta) - V_i^{exp})^2}{(\Delta V_i^{exp})^2}. \quad (9)$$

V_i^{exp} and $V_i^{th}(\zeta)$ are the experimental and theoretical (Equation 8) relaxation times T_1, T_2 or NOE

values respectively, $\Delta V_i^{\exp}$ is the uncertainty in the experimental value, N is the number of the experimentally determined relaxation rates and NOEs at different viscosities, ζ denotes a set of adjustable model parameters which are model-free parameters and the rotational correlation time τ_R. The appropriateness of a particular model can be evaluated by calculating the chi-square probability for obtaining a loss function higher or equal to the one calculated from Equation 9. Commonly, the model is taken to be inappropriate if the loss function exceeds some critical value defined by a given probability (usually the 95% quantile) for randomly obtaining a higher loss function.

If several models with different numbers of adjustable parameters have to be compared, the application of the pairwise *F*-test is very helpful (Mandel et al., 1995):

$$F(\zeta_1, \zeta_2) = \frac{\nu_2(\chi^2(\zeta_1) - \chi^2(\zeta_2))}{(\nu_1 - \nu_2)\chi^2(\zeta_2)}, \qquad (10)$$

where ζ_1 and ζ_2 denote the parameter sets for a simple and a more complex model, respectively; v_1 and v_2 ($v_1 > v_2$) are the numbers of degrees of freedom of the models. This test addresses the question of whether the reduction in the loss function obtained for a model with more parameters is statistically significant. As with the χ^2-criterion, if the value defined by Equation 10 exceeds some critical value, one must conclude that the model with more parameters is validated.

Materials and methods

Sample preparation and NMR measurements

Uniformly ^{15}N-labeled barnase was obtained as described previously (Schulga et al., 1998). The sample used for NMR spectroscopy was 1 mM ^{15}N-labeled barnase in 10 mM potassium-phosphate buffer (pH 6.4) in 95%/5% $H_2O/^2H_2O$. NMR experiments were performed on a Varian Unity (^{1}H Larmor frequency of 600 MHz) spectrometer at four glycerol concentrations: 0, 8, 16 and 20% (w/w). All experiments were conducted at 31.5 °C. A series of ^{1}H-detected two-dimensional ^{15}N–^{1}H correlation spectra for the measurements of the backbone ^{15}N longitudinal and transverse relaxation rates, and NOE were acquired using the pulse sequences described by Farrow et al. 1994. All spectra contained 1984 points in the directly detected dimension; other parameters used in the different experiments are summarized in Table 1. In ^{15}N–^{1}H NOE experiments two spectra were acquired with and without proton presaturation. Saturation was achieved by the application of ^{1}H 120° pulses spaced at 5 ms intervals for 3–5 s prior to the first ^{15}N pulse. T_2 relaxation experiments were

Table 1. Parameters of NMR relaxation experiments

Experiment	Glycerol % (w/w)	Δ (*s*)[a]	*N*[b]	Relaxation delays (ms)	*m*[c]
T_1	0	2	150	10, 40, 80, 120, 160, 240, 320, 450, 550, 700, 850, 1000	2
	8	2	150	10, 40, 80, 120, 160, 240, 320, 450, 550, 700, 850, 1000	2
	16	2	150	10, 40, 80, 120, 160, 240, 320, 450, 550, 700, 850, 1000	2
	20	2	110	10, 40, 80, 120, 160, 240, 320, 450, 550, 700, 850, 1000	2
T_2	0	2	160	16, 32, 48, 64, 80, 96, 112, 128, 144, 160, 176	2
	8	2	160	16, 32, 48, 64, 80, 96, 112, 128, 144, 160, 176	2
	16	2	160	16, 32, 48, 64, 80, 96, 112, 128, 144, 160, 176	2
	20	2	120	16, 32, 48, 64, 80, 96, 112, 128, 144, 160, 176	2
NOE	0	5	150		2
	8	5	150		2
	16	5	150		1

[a]Recovery delay.
[b]Number of complex data points acquired in the indirectly detected dimension.
[c]Number of measurements.

recorded with a CPMG echo delay of 1 ms between ^{15}N inversion pulses of 54 μs. To monitor the translational diffusion a set of 20 one-dimensional spectra (5 independent measurements for each glycerol concentration) was recorded using a slightly modified version of the spin-echo experiment (Altieri et al., 1995) with the strength of the encoding/decoding pulse field gradients (PFG) being varied in the range from 0 to ca. 30 Gs/cm. Delays of 100 ms were used for the diffusion. A relaxation delay of two seconds was used prior to each scan.

All spectra were processed and quantified in the Varian VNMR software package. A non-shifted Gaussian weighting was applied prior to the Fourier transform in the direct dimension and shifted in the indirect. Backward linear prediction for one point was used for baseline correction in directly detected dimension. Forward linear prediction in indirectly detected dimension was performed to improve resolution; time-domain data were extended up to 200 points. Peak heights were measured from the NMR spectra using routines written in the VNMR macro programming language. Relaxation rates and NOEs from several experiments were averaged in order to obtain final values.

Hydrodynamic calculations

For the evaluation of ratios D_x/D_z, D_y/D_z, Euler's angles α, β, γ and directional cosines l, m and n for the ^{15}N–^{1}H vectors (Equation 4) hydrodynamic calculations were carried out using the DIFFC module implemented in the DASHA 3.5 software package (Orekhov et al., 1996). Twenty NMR structures of barnase were taken from the Protein Data Bank (PDB entry code is 1FW7). The beads approach (Garcia de la Torre and Bloomfield, 1981) was applied for all the atoms from the united-atom force field (Weiner and Kollman, 1984). Barnase molecule was surrounded by a water shell and those water molecules for which the distance between any of its atoms and any of the protein atoms was larger than 3.2 Å were removed. A precise setting of the microscopic solvent viscosity (which scales the rotational correlation time) was not important since the effective correlation time was later adjusted through minimization of the per residue loss function. The results of the hydrodynamic calculations were used in the analysis of both synthetic and experimental relaxation data.

Model selection and determination of τ_R

It was essential to develop a special model selection strategy, required for determination of types and parameters of internal motions and to reject residues whose internal motions are potentially affected by glycerol. Thus τ_R determination protocol was developed, which consists of four stages.

In the first stage of the protocol, per residue loss function (Equation 9) minimizations are performed. During the minimization of the loss function τ_R is derived separately for each residue using relaxation data acquired at different viscosities. Rotational correlation time for the particular viscosity $\tau_{R\eta}$ is calculated from the fitted rotational correlation time for 0%-glycerol solution τ_R at every step of non-linear least squares minimization procedure using Equation 6. At this stage the parameters of rotational diffusion anisotropy (ratios D_x/D_z, D_y/D_z and Euler's angles α, β, γ) are fixed to the values taken from the hydrodynamic calculations for a given spatial structure. For internal motions, only three models are considered: model 1, model 2 and model 3 (described in the Theory section). Models 4 and 5 are not involved because it is impossible to evaluate their parameters correctly from the data acquired at one magnetic field keeping τ_R unfixed. Thus, the data at different viscosities are fitted together with two (τ_R, S^2, model 1), three (τ_R, S^2, τ_e, model 2) or four ($\tau_R, S_f^2, S_s^2, \tau_s$, model 3) adjusted parameters for each residue. The dynamic model of a particular backbone amide ^{15}N–^{1}H vector is selected according to the following method similar to the procedure proposed by Mandel et al. (Figure 1). If the value of the chi-squared probability $P(\chi^2)$ for model 1 exceeded the upper confidence level $P^{upper} = 0.2$, model 1 is taken to be appropriate. Otherwise, the experimental data are fitted with model 2 containing one additional parameter. The models are compared with the F-test (Equation 10). Provided that F-statistics probability $P(F_{1,2}) > P^{upper}$ and $P(\chi^2) > P^{upper}$ model 2 is chosen. If $P(F_{1,2})$ is less than P^{upper} the same protocol is used for model 3. Finally one of the models is selected and its χ^2 probability is compared with the lower confidence level $P^{lower} = 0.05$. The

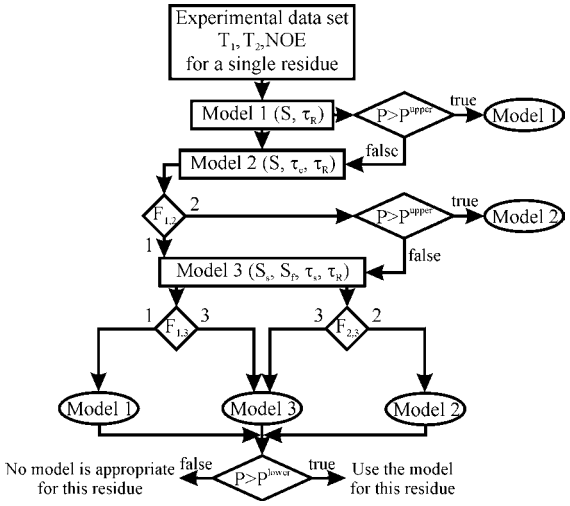

Figure 1. Flowchart of the τ_R and model selection strategy employed. Additional details provided in the text.

residue is rejected if the χ^2 probability for the selected model is smaller than P^{lower}; that may be the indication of glycerol influence upon the internal motions of the residue.

In the second stage of the protocol, the global value of τ_R is estimated through averaging values of τ_R over all accepted residues. The use of this approach became possible because rotational diffusion anisotropy has already been taken into account by application of Equation 4 with a numerically calculated rotational diffusion tensor, thus τ_R of different residues should agree within experimental uncertainty. The mean value of τ_R is used for calculation τ_{Reff} for every residue from each of 20 NMR structures (PDB entry 1FW7) using Equation 7. It allows one to reject residues whose ^{15}N–^{1}H vectors orientation is not well determined. Residues for which the value of standard deviation of τ_{Reff} is greater than 0.04 ns are omitted from further consideration. Then the mean value of τ_R is recalculated using the data from remaining residues.

In the third stage of the protocol, the residues, whose values of τ_R differing from the mean by two standard deviations, are excluded from subsequent analysis. This procedure allows one to exclude the residues data of which are possibly fitted with the wrong dynamic models and consequently with the wrong values of τ_R.

The final stage of the protocol is the simultaneous fit of all remaining experimental data for all viscosities with a value of τ_R common for all residues. At this stage, parameters of rotational diffusion anisotropy (ratios D_x/D_z, D_y/D_z and Euler's angles α, β, γ) are fitted during minimization procedure in the same manner as τ_R. Thus, we have six adjustable parameters common to the entire data set, and one, two or three additional parameters per residue depending on its dynamic model. The uncertainties of the final values of parameters are determined through covariance matrix calculation (Press et al., 1992).

All the available experimental data were processed with the above protocol. All model-free calculations were performed with a ^{15}N–^{1}H internuclear distance (R_{NH}) of 1.02 Å and a ^{15}N chemical shift anisotropy (CSA) of −170 ppm using the modified DASHA 3.5 software package for Linux (Orekhov et al., 1996).

Simulation

In order to confirm the possibility of τ_R determination from the relaxation data acquired at different viscosities we tested the above protocol on synthetic data. For each of 75 ^{15}N–^{1}H barnase spin pairs for which experimental relaxation data were collected and orientations were well defined (see below *Evaluation of the barnase overall correlation time*) 59 synthetic relaxation data sets at 3 values of $\tau_R = \{2, 6, 15\}$ ns were generated using Equations 8. For each ^{15}N–^{1}H vector its own dynamic model (from 1 to 5 described in the Theory section) and parameters of internal motions were randomly selected in order to obtain data sets with different combinations of dynamic models: from relatively rigid (models 1 and 2 over all residues) to extremely mobile (model 3 with motions in a nanosecond time scale or models 4, 5 with conformational exchange applied to each residue). Orientations of ^{15}N–^{1}H vectors and rotational diffusion tensor parameters were taken identical to those in the first structure from 1FW7 PDB entry. The values of the order parameters were S^2, S_f^2, $S_s^2 = \{0.8, 0.85, 0.9\}$. The values of the correlation times were $\tau_e = \{0.02, 0.03\}$ ns, $\tau_s = \{3, 6, 9\}$ ns. The values of the chemical exchange term were $R_{ex} = \{0.1, 0.3\}$ s^{-1}. All the relaxation data were simulated for four viscosities, which were taken equal to those used in experiments (Table 3). Gaussian random noise

was added to the simulated data with standard deviations equal to 2, 2% and 0.02 for T_1, T_2 and NOE values respectively.

Estimation of rotational diffusion from T1/T2 ratio

Protein rotational diffusion parameters are generally estimated from ^{15}N relaxation data using T_1/T_2 ratios (Tjandra et al., 1995). To compare the results of our protocol with this method we used the generally available program TENSOR (Dosset et al., 2000), which was designed for the calculation of rotational diffusion tensor from the protein spatial structure and ^{15}N T_1/T_2 ratios. The method was applied for both synthetic and experimental relaxation data. In both cases, we used the same set of 82 residues, for which relaxation data were available and NOE values exceeded 0.75. The uncertainties in the diffusion tensor components were estimated from 500 Monte-Carlo simulations using the standard procedure of the program TENSOR. The value of τ_R was calculated from the rotational diffusion tensor components according to Equation 5.

Results and discussion

Hydrodynamic calculations

Hydrodynamic calculations yielded the ratios of the principal components of the barnase diffusion tensor $D_x/D_z = 0.75$, $D_y/D_z = 0.85$ for the first structure from PDB entry 1FW7. Since all 20 barnase spatial structures from the set are very similar (mean pairwise backbone RMSD for residues 4–108 is 0.45 Å), their diffusion tensors were found to be the same within the accuracy of the computational method. The values of the ratios D_x/D_z and D_y/D_z along with the direction cosines l, m and n of each ^{15}N–^{1}H vector for the first structure from PDB entry 1FW7 were used both in simulation studies and in the evaluation of τ_R from experimental relaxation rates at the first stage of the protocol. At the final stage of the protocol, when all the components of the diffusion tensor were fitted using the experimental data, the direction cosines of each ^{15}N–^{1}H vector were also taken from the first structure.

Simulation

In general, the model selection algorithm (Figure 1) adequately predicts dynamic models and correctly determines their parameters in the case of simulation with models 1 and 2 (internal motions in picosecond time scale). For simulations with model 3 the model selection algorithm erroneously predicts model 1 or 2 when relaxation data are simulated with $\tau_R = 2$ ns and works well for $\tau_R = 15$ ns. For the data simulated with $\tau_R = 6$ ns dynamic model 3 is correctly reproduced by the prediction algorithm in about 50% of cases depending on τ_s and order parameters values. Wrong prediction of model 1 or 2 instead of the actually assigned model 3 can be explained by a too narrow viscosity range (Table 3) that is insufficient to τ_R to exceed τ_s even at the maximum of viscosity. Another reason is the high value of the order parameter S_s^2 of internal motions in nanosecond time scale. When the value of S_s^2 is equal to 0.85 or higher, the model selection algorithm often selects simpler models 1 or 2 as more statistically significant. The selection of model 1 or 2 instead of model 3 leads to underestimated values of τ_R as a result of a fitting procedure in agreement with previous studies (Korzhnev et al., 1997).

When relaxation data are simulated with model 4 or 5 (fast internal motions in picosecond time scale along with chemical exchange term R_{ex} added to transverse relaxation rate), the model selection algorithm selects model 1 or 2 since it is impossible to determine the parameters of models 4 and 5 keeping τ_R unfixed. This leads to slightly overestimated values of τ_R as a result of the fitting procedure.

Despite of the difficulties described above, the τ_R determination method gives final τ_R esteems in good agreement with assigned values. The estimated value deviates from the assigned one by no more than 5% in almost all the cases except several data sets simulated with the only model 3 (all protein residues are involved in motions in nanosecond time scale) or with the exchange term R_{ex} applied to each residue. Some results of the τ_R determination method for synthetic data are summarised in Table 2. In general, the values of the overall rotational correlation time calculated according to our protocol are closer to the assigned values than τ_R obtained from T_1/T_2 ratios. The most considerable difference in these

Table 2. Some results of testing of τ_R determination protocol on synthetic data

Data set number	Percentage of residues simulated with the following models of internal motions					τ_R obtained with our protocol (τ_R determined from T_1/T_2 ratio)		
	1	2	3	4	5	$\tau_R = 2$ ns	$\tau_R = 6$ ns	$\tau_R = 15$ ns
1	18.2	18.2	27.3	18.2	18.2	2.002 ± 0.006 (2.05 ± 0.02)	6.00 ± 0.01 (5.85 ± 0.02)	15.02 ± 0.02 (13.81 ± 0.05)
2	50	50	–	–	–	1.996 ± 0.005 (2.01 ± 0.02)	6.00 ± 0.02 (5.97 ± 0.03)	15.00 ± 0.02 (14.85 ± 0.05)
3	50	–	50	–	–	1.962 ± 0.005 (1.97 ± 0.02)	5.82 ± 0.02 (5.69 ± 0.02)	15.01 ± 0.02 (13.13 ± 0.04)
4	33.3	33.3	33.3	–	–	1.968 ± 0.005 (1.98 ± 0.02)	5.91 ± 0.01 (5.77 ± 0.02)	14.99 ± 0.02 (13.49 ± 0.05)
5	33	–	–	66	–	2.054 ± 0.006 (2.14 ± 0.02)	6.05 ± 0.01 (6.05 ± 0.03)	15.05 ± 0.02 (15.00 ± 0.06)
6	–	50	–	50	–	2.040 ± 0.006 (2.10 ± 0.02)	6.03 ± 0.01 (6.02 ± 0.02)	15.03 ± 0.02 (14.89 ± 0.06)
7	25	25	25	25	–	1.993 ± 0.006 (2.03 ± 0.02)	6.03 ± 0.01 (5.84 ± 0.03)	15.03 ± 0.02 (13.84 ± 0.05)
8	33.3	66.6	–	–	–	1.992 ± 0.005 (2.00 ± 0.02)	6.00 ± 0.01 (5.96 ± 0.03)	15.00 ± 0.02 (14.81 ± 0.06)
9	–	66.6	33.3	–	–	1.959 ± 0.005 (1.98 ± 0.02)	5.91 ± 0.01 (5.75 ± 0.03)	14.99 ± 0.02 (13.46 ± 0.05)
10	25	50	25	–	–	1.973 ± 0.006 (1.98 ± 0.02)	6.01 ± 0.01 (5.82 ± 0.02)	15.02 ± 0.02 (13.82 ± 0.05)
11	50	–	–	–	50	2.032 ± 0.006 (2.10 ± 0.02)	6.03 ± 0.01 (6.02 ± 0.03)	15.03 ± 0.02 (14.88 ± 0.06)
12	–	50	–	–	50	2.025 ± 0.006 (2.09 ± 0.03)	6.03 ± 0.01 (6.00 ± 0.03)	15.03 ± 0.02 (14.78 ± 0.05)
13	33.3	–	66.6	–	–	1.948 ± 0.005 (1.96 ± 0.02)	5.72 ± 0.02 (5.61 ± 0.02)	14.97 ± 0.03 (12.76 ± 0.05)
14	–	33.3	66.6	–	–	1.935 ± 0.005 (1.95 ± 0.02)	5.71 ± 0.02 (5.60 ± 0.02)	14.97 ± 0.03 (12.73 ± 0.05)
15	28.6	28.6	42.9	–	–	1.950 ± 0.005 (1.96 ± 0.02)	5.77 ± 0.02 (5.64 ± 0.03)	14.98 ± 0.02 (12.88 ± 0.05)

Note: The values within parenthesis represents τ_R determined from T_1/T_2.

values is observed when more than 40% of ^{15}N–^{1}H vectors are involved in internal motions in nanosecond time scale (data sets number 3, 13–15 simulated with $\tau_R = 6$ and 15 ns). The presence of a great number of ^{15}N–^{1}H vectors with conformational exchange (5, 6, 11 and 12 data sets) leads to systematically overestimated values of τ_R, which however are in a good correspondence with the assigned values. For $\tau_R = 2$ ns both approaches show similar results in agreement with previous studies (Korzhnev et al., 1997). It is noteworthy that for models with more than 30% of ^{15}N–^{1}H vectors having motions in nanosecond time scale (data sets number 3, 4, 9, 13–15) and $\tau_R = 6$ ns there is a considerable discrepancy between overall correlation times assigned in simulation and determined using our protocol, which substantially exceeds the estimated uncertainty. A possible explanation of too small uncertainty of τ_R is that the method used for the calculation of the uncertainty does not account for the mismatch between the theory and the experiment. When the theoretical model matches experimental data, the method gives the correct value of the uncertainty of τ_R. However, in the case of a wrong fit with high χ^2 value the method gives too

low uncertainties. In the case of $\tau_R = 6$ ns for data sets 3, 13–15, χ^2 value exceeds 2200 for about 700 degrees of freedom leading to the incorrect determination of τ_R and its uncertainty. However, when the number of residues with nanosecond internal motions is lower than 30% (data sets number 1, 7, 10), the value of χ^2 drops to 1000 or lower and the value of τ_R is determined correctly. It is clear from Table 2 that the use of our approach leads to a more correct evaluation of τ_R than the value obtained from T_1/T_2 ratios, especially when the major part of the residues is involved in slow motions. Apparently, our protocol is applicable to evaluation of rotational diffusion.

NMR measurements

Of the 106 backbone amide groups of barnase, 88 were included in the relaxation measurements. Seven cross peaks were missed in the spectra (GLN2, SER38, ARG59, SER67, GLY68 and ILE109), for ALA37, ASN58 and GLU60 cross peaks were too weak, i.e., their signal-to-noise ratio was less than 20. Four pairs of peaks were significantly overlapped (SER28 and GLY52, ALA30 and ASP54, TYR78 and ASN84, ILE96 and HIS102) and therefore excluded from analysis. As it was expected, the addition of glycerol diminished the signal-to-noise ratio but no more than by 50%. The signal-to-noise ratio varied from signal to signal and from one experiment to another, but was never less than 40 (even for the highest glycerol concentration used). This resulted in very small, usually less than 1% uncertainties of T_1 and T_2 values obtained in the exponential fitting procedure. The mean values of ^{15}N T_1, T_2 and NOE along with their uncertainties are shown in Figure 2. The addition of glycerol leads to an increase in T_1 and decrease in T_2, leaving NOE values almost unchanged, as was expected from the simulation.

Values of the translation diffusion coefficient obtained in PFG NMR measurements are presented in Table 3. Estimated errors in diffusion experiments were less than 0.5%. As one can see from Table 3, the translation diffusion coefficient is almost twofold bigger at 0% (w/w) glycerol concentration than at 20%. In the simulations we showed that in most cases this range is sufficient for the correct evaluation of τ_R.

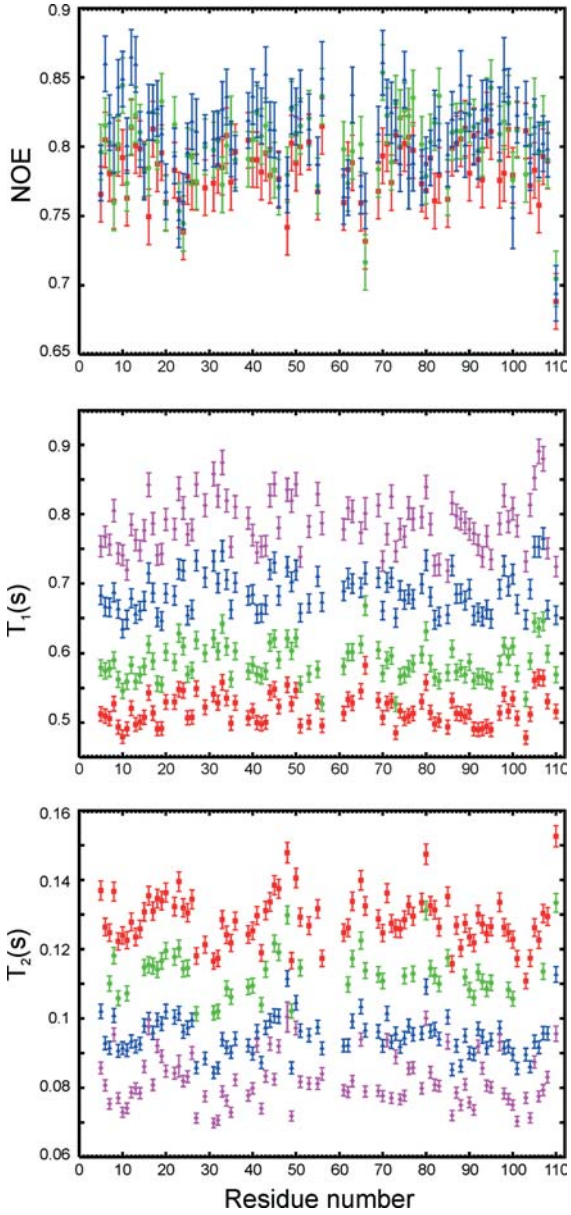

Figure 2. Relaxation data as a function of residue for barnase. Red squares, green circles, blue triangles and magenta rhombuses are for 0, 8, 16 and 20% glycerol percentage ratios respectively. The data for the residues 3 and 4 are out of scale and not present on the figure.

For several residues the linear dependence of ^1H and ^{15}N chemical shifts on viscosity of the solution was noticed (data not shown). However, the differences in chemical shifts ($\Delta\delta$) for these residues in aqueous and most viscous solutions were not dramatic, usually $\Delta\delta < 0.03$ ppm for

Table 3. Dependence of diffusion parameters of barnase on viscosity

Glycerol (w/w) %	$D_{t\eta}$ (10^{-10} m^2/s)[a]	$D_t/D_{t\eta}$[b]	$\tau_{R\eta}$ (ns)[c]	τ_R $D_t/D_{t\eta}$ (ns)[d]
0	1.428 ± 0.004	1	5.51 ± 0.03	5.56 ± 0.01
8	1.201 ± 0.005	1.189	6.55 ± 0.03	6.61 ± 0.04
16	0.989 ± 0.005	1.444	8.01 ± 0.04	8.03 ± 0.05
20	0.829 ± 0.002	1.721	9.39 ± 0.05	9.57 ± 0.06

[a]The translational diffusion coefficient determined by PFG NMR experiments.
[b]The ratio of translational diffusion coefficients of aqueous (D_t) and glycerol containing ($D_{t\eta}$) solutions.
[c]The overall rotational correlation time at different viscosities determined from T_1/T_2 ratio by the program Tensor.
[d]The overall rotational correlation time at different viscosities determined by Equation 6.

^1H, $\Delta\delta < 0.3$ ppm for ^{15}N. It means that the structure of the protein was not strongly influenced by glycerol.

Evaluation of the barnase overall correlation time

At the first stage of the protocol (Figure 1) data of 10 ^{15}N–^1H vectors with too low χ^2 probability (i.e. their chi-square probability was below the 0.05 threshold) were rejected (Figure 3d). At the second stage of the protocol preliminary value of τ_R was estimated and used to calculate τ_{Reff} (see Equation 5) for 20 NMR structures. Then the data of 13 residues for which the standard deviation of τ_{Reff} was greater, than 0.04 ns, were excluded due to the poorly defined orientations of their ^{15}N–^1H vectors (Figure 3b). This value of cut-off (0.04 ns) is twice as much as the value of τ_R uncertainty obtained in simulation for $\tau_R = 6$ ns (Table 2), so using the data of these ^{15}N–^1H vectors could result in a large error in the calculated value of τ_R.

At the third stage 3 residues (ILE4, ASP101, ARG110) whose τ_R were out of the interval $(<\tau_R> - 2\sigma, <\tau_R> + 2\sigma)$, where $<\tau_R>$ is the mean value of τ_R ($<\tau_R> = 5.55$ ns) and $\sigma = 0.17$ ns is the standard deviation, were excluded (Figure 3c). Thus far, the internal motions of only 13 ^{15}N–^1H vectors were probably altered with glycerol and consequently excluded from the following data analysis. Of 88 backbone amide groups, whose relaxation data were evaluated in the NMR measurements, 62 groups were included in the final relaxation data set used for τ_R calculations. As one can see from Figure 3a, the final set of residues is uniformly distributed over the entire barnase spatial structure covering various structural elements.

The final stage was the simultaneous fit of the final relaxation data set with the global rotational diffusion parameters. The cumulative loss function over the final data set was 776 for 606 degrees of freedom. As it was shown on synthetic data, such a value of χ^2 usually corresponds to a good match between the theory and the experiment. The global τ_R obtained for the 62 backbone amide groups was 5.56 ± 0.01 ns and the ratios of the principal components of the barnase diffusion tensor $D_x/D_z = 0.76 \pm 0.01$, $D_y/D_z = 0.80 \pm 0.01$.

The barnase relaxation data at different viscosities were also processed by program TENSOR. The ratios of the principal components of the barnase diffusion tensor determined from the relaxation data were $D_x/D_z = 0.78 \pm 0.01$ and $D_y/D_z = 0.85 \pm 0.01$ for 0%-glycerol solution. These values are in good agreement both with the values obtained using the proposed protocol and with the theoretical hydrodynamic calculations ($D_x/D_z = 0.75$, $D_y/D_z = 0.85$) used at the first stage of the protocol. The overall rotational correlation times reported by the program TENSOR for different viscosities $\tau_{R\eta}$ are presented in Table 3. They are also in good correspondence with the values of $\tau_{R\eta}$ determined by our protocol (rightmost column in Table 3). This result is not surprising because only models 1 and 2 were used to fit the relaxation data for all the 62 residues during the determination of τ_R (Figures 3c,d). As it was shown on the synthetic data, in this case both the methods give very similar results. A conformance between $\tau_{R\eta}$ values obtained by these methods also indicates appropriateness of Equation 6 used in the proposed protocol for the estimation of $\tau_{R\eta}$ from τ_R and translational diffusion coefficients.

Conclusions

We have shown the possibility of a joined fit of NMR relaxation data acquired at different viscosities. The relaxation data analysis allows unambiguous determination of a protein overall rotational correlation time. The elaborated

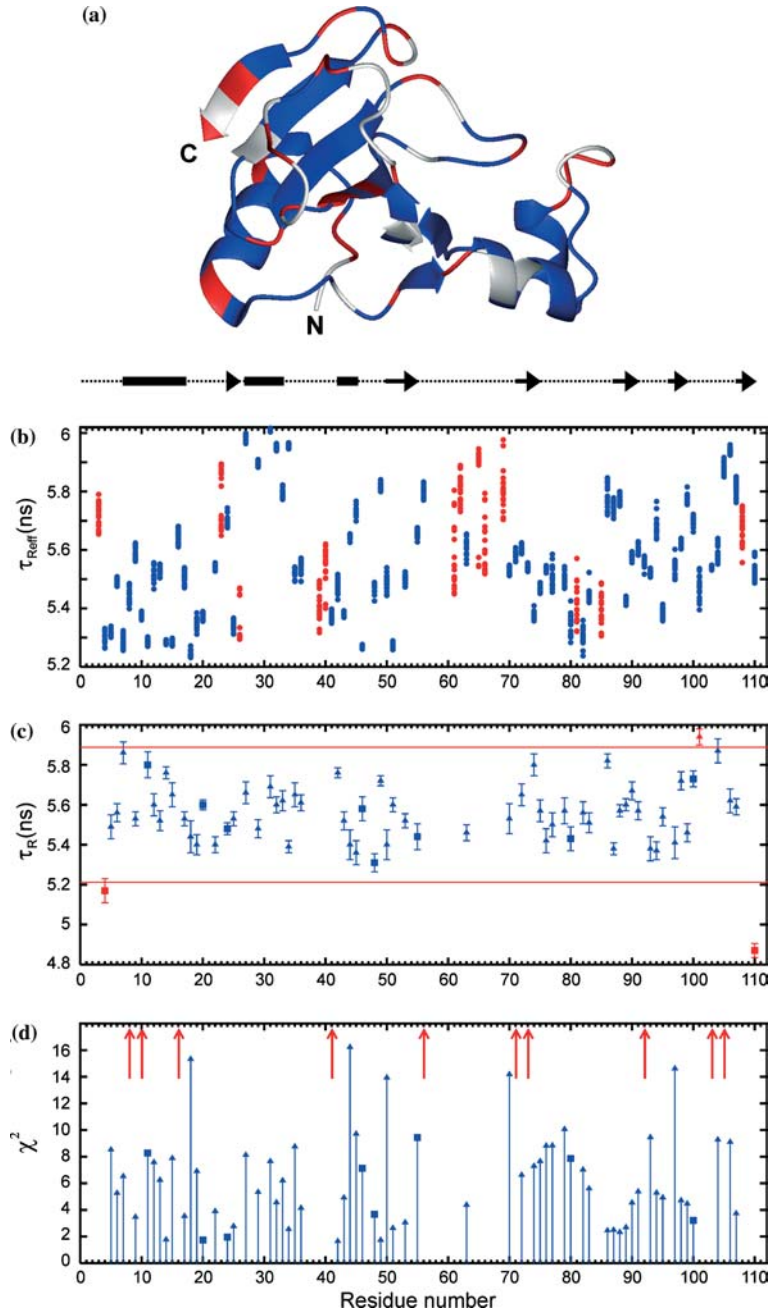

Figure 3. Determination of overall rotational correlation time for barnase. (a) The ribbon diagram of barnase spatial structure. The blue colour is for residues from the final data set used for calculation of τ_R. The red colour represents residues whose data were excluded from final data set due to various reasons. The residues without relaxation data are shown in grey. The figure was produced with the MOLMOL program (Koradi et al., 1996). (b) The effective rotational correlation time τ_{Reff} calculated for each residue in 20 structures of barnase (PDB entry 1FW7). The red data points represent residues, which were excluded from analysis due to poorly defined orientations of their ^{15}N–^{1}H vectors. (c) The overall rotational correlation time calculated for each residue. The filled triangles are for model 1, filled squares are for model 2. The lines bounding $\pm 2\sigma$ interval and the data points out of this interval are shown in red. (d) The penalty function values after per residue fit of τ_R. The squares and the triangles are the same as in the previous graph. The red arrows represent residues, which were excluded due to the χ^2 criterion.

approach displayed its efficiency in comprehensive tests on synthetic relaxation data: τ_R is determined correctly even if ^{15}N–^{1}H vectors undergo nanosecond internal motions.

NMR relaxation experiments with ribonuclease barnase and glycerol confirmed the applicability of the method to globular proteins. The overall rotational correlation time $\tau_R = 5.56 \pm 0.01$ ns calculated for barnase according to our approach correlate well with that obtained from T_1/T_2 ratios. This fact indicates that barnase internal motions, which contribute to the relaxation rates, take place predominantly in a fast picosecond time scale. Although our consideration was based on the model-free approach, which implies uncorrelated internal and overall motions, the good correspondence between the theory and experiment in the case of barnase indicates the independence of internal motions from overall rotation.

Acknowledgements

This work was supported in part by the Program RAS MCB and by the Ministry for Science and Technology of the Russian Federation (SS-1522.2003.4).

References

Abragam, A. (1961) *The Principles of Nuclear Magnetism*, Clarendon Press, Oxford.

Altieri, A.S., Hinton, D.P. and Byrd, R.A. (1995) *J. Am. Chem. Soc.*, **117**, 7566–7567.

Clore, G.M., Szabo, A., Bax, A., Kay, L.E., Driscoll, P.C. and Gronenborn, A.M. (1990) *J. Am. Chem. Soc.*, **112**, 4989–4991.

Dosset, P., Hus, J.C., Blackledge, M. and Marion, D. (2000) *J. Biomol. NMR*, **16**, 23–28.

Farrow, N.A., Muhandiram, R., Singer, A.U., Pascal, S.M., Kay, C.M., Gish, G., Shoelson, S.E., Pawson, T., Forman-Kay, J.D. and Kay, L.E. (1994) *Biochemistry*, **33**, 5984–6003.

Garcia de la Torre, J. and Bloomfield, V.A. (1981) *Quart. Rev. Biophys.*, **14**, 81–139.

Hartley, R.W. (1997) In *Ribonucleases. Structures and Functions*, D'Alessio, G. and Riordan, J.F. (Eds.), Academic Press, New York, pp. 51–100.

Koradi, R., Billeter, M. and Wüthrich, K. (1996) *J. Mol. Graph.*, **14**, 51–55.

Korzhnev, D.M., Billeter, M., Arseniev, A.S. and Orekhov, V. Yu. (2001) *Prog. Nucl. Magn. Reson. Spectrosc.*, **38**, 187–266.

Korzhnev, D.M., Orekhov, V.Yu. and Arseniev, A.S. (1997) *J. Magn. Reson.*, **127**, 184–191.

Lipary, G. and Szabo, A. (1982) *J. Am. Chem. Soc.*, **104**, 4546–4559.

Mandel, A.M., Akke, M. and Palmer, A.G. (1995) *J. Mol. Biol.*, **246**, 144–163.

Orekhov, V.Yu., Dubovskii, P.V., Yamada, H., Akasaka, K. and Arseniev, A.S. (2000) *J. Biomol. NMR*, **17**, 257–263.

Orekhov, V.Yu., Korzhnev, D.M., Pervushin, K.V., Hoffmann, E. and Arseniev, A.S. (1999) *J. Biomol. Struct. Dyn.,* **17**, 157–174.

Orekhov, V.Yu., Nolde, D.E., Golovanov, A.P., Korzhnev, D.M. and Arseniev, A.S. (1996) *Appl. Magn. Reson.*, **9**, 581–588.

Press, W.H., Teukolsky, S.A., Vetterling, W.T. and Flannery, B.P. (1992) *Numerical Recipes in FORTRAN*, Cambridge University Press, Cambridge.

Schulga, A., Kurbanov, F., Kirpichnikov, M., Protasevich, I., Lobachev, V., Ranjbar, B., Chekhov, V., Polyakov, K., Engelborghs, Y. and Makarov A. (1998) *Protein Eng.*, **11**, 773–780.

Tjandra, N., Feller, S.E., Pastor R.W. and Bax, A. (1995) *J. Am. Chem. Soc.*, **117**, 12562–12566.

Tugarinov, V., Liang, Z., Shapiro Y.E., Freed, J.F. and Meirovitch, E. (2001) *J. Am. Chem. Soc.*, **123**, 3055–3063.

Weiner, S.J., Kollman P.A. and Weiner, P. (1984) *J. Am. Chem. Soc.*, **106**, 765–784.

Woessner, D.E. (1962) *J. Chem. Phys.*, **37**, 647–654.

Zeeb, M., Jacob, M.H., Schindler, T. and Balbach, J. (2003) *J. Biomol. NMR*, **27**, 221–234.